Fuel 148 (2015) 48–57

Contents lists available at ScienceDirect

Fuel

journal homepage: www.elsevier.com/locate/fuel

Hierarchical zeolite Y supported cobalt bifunctional catalyst for facilely tuning the product distribution of Fischer–Tropsch synthesis

Chuang Xing [a,b], Guohui Yang [b], Mingbo Wu [c], Ruiqin Yang [a], Li Tan [b], Pengfei Zhu [b], Qinhong Wei [b], Jie Li [b], Jianwei Mao [a], Yoshiharu Yoneyama [b], Noritatsu Tsubaki [a,b,*]

[a] Zhejiang Provincial Key Lab for Chem. & Bio. Processing Technology of Farm Product, School of Biological and Chemical Engineering, Zhejiang University of Science and Technology, Hangzhou 310023, PR China
[b] Department of Applied Chemistry, Graduate School of Engineering, University of Toyama, Gofuku 3190, Toyama 9308555, Japan
[c] State Key Laboratory of Heavy Oil Processing, China University of Petroleum, Qingdao 266580, PR China

HIGHLIGHTS

- Hierarchical zeolite Y is prepared by the sequential leaching process.
- The mesopore volume increases after the sequential treatment.
- Low methane selectivity and excellent high isoparaffin selectivity are achieved.
- Better catalytic performance is attributed to the combine acidity and mesoporisity.

GRAPHICAL ABSTRACT

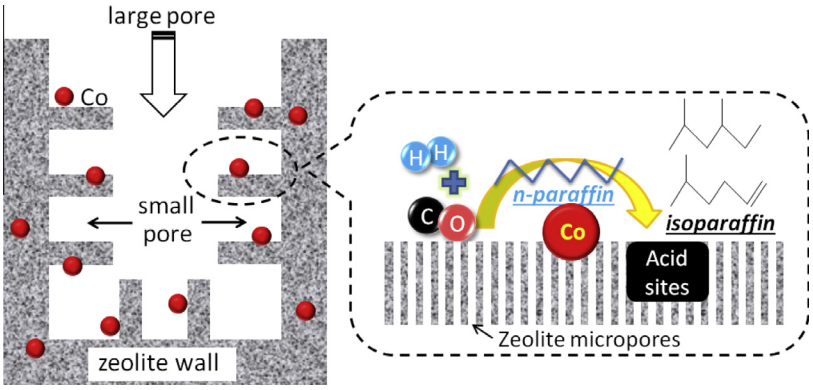

ARTICLE INFO

Article history:
Received 28 August 2014
Received in revised form 10 December 2014
Accepted 15 January 2015
Available online 7 February 2015

Keywords:
Fischer–Tropsch synthesis
Isoparaffin
Hierarchical
Zeolite Y
Mesopore

ABSTRACT

A two-step method consisting of acid leaching and base leaching was developed and applied to create hierarchical pores on a general microporous Y zeolite. Characterization with BET and TEM on the texture, morphology and structure of the prepared hierarchical Y zeolite confirmed the co-existence of mesopores with zeolitic walls. The analysis results showed that the mesopore surface area and pore volume of the hierarchical zeolite Y (Y-AB*x*, A: acid leaching, B: base leaching, "*x*" represents for base leaching time) increased with increasing the base leaching time. The hierarchical zeolite Y supported Co as catalysts were employed to catalyze the hydrogenation of carbon monoxide to form hydrocarbons through Fischer–Tropsch synthesis (FTS) reaction. The CO conversion and C_{5-11} selectivity on Co/Y-AB*x* catalysts increased significantly compared with those on the pristine Y supported Co catalyst. The isoparaffin selectivity of Co/Y-AB4 catalyst reached up to 52.3% and middle hydrocarbons became the main FTS products due to the optimized hydrocracking and isomerization function afforded by the hierarchical zeolite Y with the strong Brønsted acid/Lewis acid (B/L) ratio and textural property.

1. Introduction

Zeolite, with unique micropore structure, high thermal stability and high acidity, is widely applied as adsorbent, catalyst or catalyst

* Corresponding author at: Department of Applied Chemistry, Graduate School of Engineering, University of Toyama, Gofuku 3190, Toyama 9308555, Japan. Tel./fax: +81 76 445 6846.
E-mail address: tsubaki@eng.u-toyama.ac.jp (N. Tsubaki).

http://dx.doi.org/10.1016/j.fuel.2015.01.040
0016-2361/

supports in lots of fields, such as basic petrochemistry, oil refining and fine chemicals synthesis [1–3]. In general, the pore size and cavities of the zeolite are less than 0.8 nm and 1.5 nm, respectively [4,5]. Therefore, the narrow zeolite pores and channels lead to severe transport limitation for reactants and products in catalytic reactions [6–9].

In order to overcome this disadvantage, a new concept of hierarchical zeolite with the combined mesopores and zeolitic microporous walls, as highly active catalyst, has been presented in recent years [10,11]. The general preparation methods for the hierarchical zeolite production are steaming, acid leaching (dealumination), base leaching (desilication) or templating [7,12]. Sasaki et al. reported that the dealumination led to the formation of mesoporous channels [13]. More recently, various carbon templates were also used to introduce mesopores into microporous zeolite [14–20]. For application of mesoporous zeolite-based catalysts, Bao and co-workers demonstrated that Mo loaded on mesoporous ZSM-5 catalyst showed excellent catalytic performance for methane aromatization [21]. Li et al. proved that the mesoporous mordenite had better catalytic activity than untreated microporous mordenite in the alkylation of benzene with benzyl alcohol [22]. The desilicated ZSM-5 zeolite supported metal catalyst for direct gasoline synthesis from syngas exhibited good activity [23–25]. Wang et al. reported direct isoparaffin synthesis with high selectivity through the mesoporous ZSM-5 supported noble metal catalyst in Fischer–Tropsch synthesis (FTS). However, the noble metal catalyst with small loading amount could not exhibit considerably higher reaction activity if compared with the low cost iron and cobalt-based FTS catalysts [26].

FTS reaction is a promising process to produce ultra clean liquid fuel by CO hydrogenation, and it is also an important route to deal with the recent oil crisis and environment problems [27–31]. The general FTS products are linear paraffin with little α-olefin, and their distribution strictly follows the Anderson–Schulz–Flory (ASF) law [23,24,32,33]. As well known, the pore structure and acidity of catalyst support can affect FTS reaction rate and product distribution. Recently, with zeolite as FTS catalyst supports, some researchers have devoted to synthesizing hydrocarbons in a narrow distribution, especially in the range of gasoline [33–37]. Zeolite Y with the faujasite (FAU) structure is an excellent catalyst for cracking reaction. It has been extensively used in fluid catalytic cracking (FCC) process [38–40]. However, its catalytic reaction rate is limited severely by the microporous channels of zeolite Y [7]. Therefore, the development of zeolite Y catalysts with mesoporous cavities is also necessary.

In this paper, we designed a hierarchical zeolite Y supported cobalt catalyst for tuning the selectivity of FTS products. The hierarchical zeolite Y, simultaneously containing micropores and mesopores, was facilely prepared using an acid leaching and a followed by base leaching procedures. The acid leaching on zeolite Y not only enhanced its structure stability, but also improved its catalytic activity. In addition, the followed base leaching could partly remove some silicon from zeolite framework, forming the desired mesoporous structure. For the cobalt loaded on hierarchical zeolite Y catalyst, the micropores of zeolite could provide large surface area, high cobalt dispersion as well as rich acid sites, while the mesoporous structure would facilitate the diffusion of reactants and products in FTS reaction.

2. Experimental section

2.1. Catalyst preparation

The hierarchical zeolite Y was obtained by a sequential dealumination and desilication process with the assistance of acid leaching plus base leaching. The overall synthetic route is illustrated in Fig. 1. The pristine zeolite Y (Y-P zeolite, Si/Al = 3.05, TOSOH CO.) was first treated with 0.17 M citric acid solution at 80 °C for 4 h, subsequently washed with deionized water, dried at 120 °C overnight and calcined in air at 550 °C for 3 h. The obtained sample was denoted as Y-A.

The dealuminized zeolite Y (Y-A) was further leached with 0.1 M NaOH aqueous solution for 0.25, 1, 4 and 6 h, respectively. The sample was filtered, washed with deionized water, dried at 120 °C overnight and calcined in air at 550 °C for 3 h. Finally, the obtained zeolite sample was exchanged in $NH_4{\cdot}NO_3$ solution at 80 °C for certain time, and then calcined at 550 °C for 5 h to get H-type hierarchical zeolite Y. The hierarchical zeolite Y was denoted as Y-AB*x* (A: acid leaching, B: base leaching, *x* = 0.25, 1, 4 and 6) where the "*x*" stands for the leaching time by NaOH solution.

Another reference catalyst without acid leaching but with base leaching had also been prepared. The base leaching time on the pristine zeolite Y was 1 h, followed by the same procedure to the above mentioned base leaching method. The final catalyst was named as Y-B.

The FTS catalysts with cobalt loading amount of 10 wt% were prepared by an incipient wetness impregnation (IWI) method with the prepared zeolite Y-A, Y-B and hierarchical Y-AB*x* as catalyst supports. The cobalt came from an aqueous solution of cobalt nitrate. Finally, the wet catalyst was dried at 120 °C overnight and then calcined in air at 400 °C for 2 h. These catalysts were named Co/Y-A, Co/Y-B and Co/Y-AB*x* (*x* = 0.25, 1, 4 or 6), respectively. The pristine zeolite Y supported cobalt catalyst, as a reference catalyst, was also prepared by IWI method and denoted as Co/Y-P.

2.2. Catalyst characterization

The crystalline structure of the zeolite samples was measured by X-ray diffraction (XRD) with a Rigaku RINT 2400 diffractometer employing Cu Kα radiation. All samples were scanned at 40 kV and 40 mA. The relative crystallinity (the percentage of crystalline material) of the zeolite was also determined by X-ray diffraction. The relative crystallinity was determined by comparing the diffraction intensities of the three major peaks at 2θ = 6.2, 15.6, and 23.6. The relative crystallinity was calculated using equation: Cryst (%) = $\alpha_0 \times I/I_0$, where Cryst (%) and α_0 are the crystallinities of the unknown and pristine zeolite Y (defined 100%), respectively, and I and I_0 are the heights of the characteristic peaks of the unknown and pristine zeolite Y, respectively.

The Si/Al molar ratio of the zeolite samples was determined by an energy dispersive X-ray spectroscopy (EDX-700, Shimadzu).

Transmission electron microscopy (TEM) measurements were performed on JEOL JEM-2100 UHR at an acceleration voltage of 200 kV to analyze the morphology of zeolite samples.

The nitrogen adsorption and desorption measurements of the zeolite samples were performed on a Micromeritics 3Flex analyzer (Micromeritics Instrument CO.). The surface area of samples was determined by the Brunauer–Emmett–Teller (BET) method. The pore size distribution of micropore was determined by HK method. The pore size distribution of mesopores was obtained from desorption branch by the Barrett–Joyner–Halenda (BJH) method. The surface area and volume of micropores were determined by the *t*-plot method. Mesoporous surface area was also evaluated by the *t*-plot method.

Pyridine IR (Py-IR) spectra were conducted on FT-IR spectrometer. For the Py-IR experiment, the sample was placed into self-supported wafers in an in situ IR cell. Sample was first evacuated at 350 °C for 3 h under a vacuum of 10^{-2} Pa, and then cooled to room temperature, followed by adsorption of purified pyridine

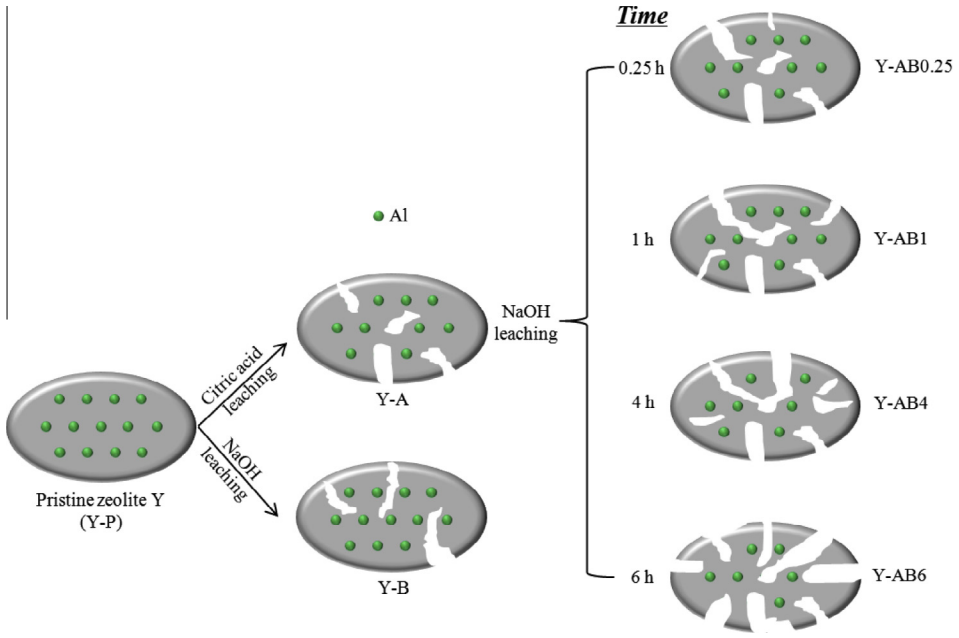

Fig. 1. Schematic depiction of the hierarchical zeolite Y preparation procedure.

vapor for 30 min. The excess pyridine was removed at 150 °C for 1 h under the vacuum, and the Py-IR spectra were collected after the temperature reduced to room temperature. The system was also evacuated at 350 °C, and IR spectra were recorded. The Brønsted acid/Lewis acid (B/L) ratio was calculated by previous report [41].

H_2 temperature programmed reduction (H_2-TPR) and NH_3 temperature programmed desorption (NH_3-TPD) experiments were performed in a flow apparatus on a BELCAT-B-TT (BEL CO.) instrument. In a typical H_2-TPR experiment, 0.03 g of catalyst was pretreated at 150 °C in a quartz-made tube under a flowing He for 1 h, followed by cooling to 50 °C. Then, H_2/Ar mixture (5%H_2, 20 mL/min) was introduced into the tube, and the temperature was linearly increased from 150 °C to 500 °C with a heating rate of 5 °C/min. The consumption of H_2 was detected by gas chromatograph with a thermal conductivity detector (TCD).

For the NH_3-TPD analysis, the catalyst was first loaded in a quartz-made tube and then pretreated in the flowing He at 150 °C for 1 h. The adsorption process was performed by using 5%NH_3 in He with a flow rate of 20 mL/min at 80 °C for 20 min. The primary desorption process proceeded first on the NH_3-saturated catalyst at 80 °C under flowing He for 1 h to remove some physically adsorbed NH_3, and then the NH_3-TPD was implemented by increasing the temperature from 100 °C to 500 °C at the heating rate of 5 °C/min in He (20 mL/min).

2.3. FTS reaction

FTS reaction was carried out in a flowing fixed-bed reactor at 260 °C under reaction pressure of 1.0 MPa. In brief, 0.5 g catalyst was loaded in the middle of the stainless steel reactor and reduced in situ at 400 °C in a flow of pure H_2 (80 mL/min) for 10 h prior to reaction. FTS reaction was implemented using syngas with the ratio of H_2/CO = 2 and the $W_{Catalyst}/F_{Syngas}$ = 10 gh/mol. An ice trap with octane as solvent was fixed between reactor and back pressure regulator to capture the heavy hydrocarbons. The obtained heavy hydrocarbons were finally analyzed by an offline gas chromatograph (Shimadzu GC-2014, FID). The residual gaseous products effused from the ice trap were analyzed online by other two online gas chromatographs (Shimadzu GC-8A, TCD and Shimadzu GC-14B, FID).

3. Results and discussion

The XRD patterns of the zeolite samples are illustrated in Fig. 2. All of the samples exhibit similar peaks with the faujasite zeolite diffraction pattern. The crystallization intensity of the treated zeolite Y with acid (Y-A), base (Y-B) or the combination of acid and base (Y-AB*x*) is weaker than that of the pristine zeolite Y (Y-P). The relative crystallinity of all of the zeolite samples is also determined by XRD and listed in Table 1, where we can find that the crystallinity of samples after acid leaching, base leaching or the combined acid and base leaching decreases in comparison with that of the pristine zeolite Y-P. The lowest zeolite crystallinity is 48.3% for Y-AB6 sample, indicating that the base leaching for 6 h possibly leads to the partial collapse of zeolite structure [4,42,43].

The nitrogen adsorption and desorption isotherms of the Y-P and hierarchical zeolite samples are shown in Fig. 3. The isotherm slopes of the hierarchical zeolite samples are larger than that of the pristine Y-P zeolite, indicating the formation of mesopores after leaching process. For Y-A sample obtained by single acid leaching, its hysteresis loop enlarges slightly compared with the pristine zeolite Y-P. It is interesting that the scope of the hysteresis loop

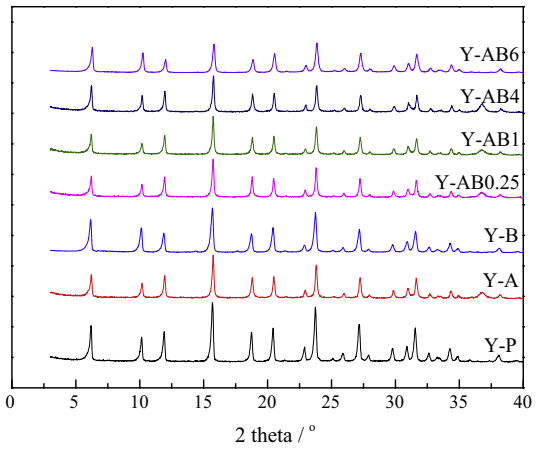

Fig. 2. XRD patterns of Y-P and hierarchical zeolite samples.

Table 1
Summary of the textural properties of different samples.

Sample	S (m^2/g)[a]			V (cm^3/g)			Si/Al ratio[g]	%Cryst[h]
	Total	Micro[b]	Meso[c]	Total[d]	Micro[e]	Meso[f]		
Y-P	589	528	61	0.38	0.28	0.10	3.04	100.0
Y-A	628	557	71	0.45	0.31	0.15	4.92	75.9
Y-B	643	564	79	0.43	0.30	0.13	2.84	82.8
Y-AB0.25	638	563	75	0.46	0.28	0.18	4.72	65.5
Y-AB1	619	541	78	0.48	0.28	0.20	4.69	63.4
Y-AB4	615	530	85	0.52	0.28	0.24	4.32	58.1
Y-AB6	607	509	98	0.57	0.28	0.29	4.05	48.3

[a] BET surface area.
[b] Microporous surface area evaluated by the *t*-plot method.
[c] Mesoporous surface area evaluated by the *t*-plot method.
[d] Total pore volume calculated by single point method at $P/P_0 = 0.99$.
[e] Micropore volume evaluated by the *t*-plot method.
[f] Mesopore volume calculated as $V_{Meso} = V_{Total} - V_{Micro}$.
[g] Si/Al mole ration determined by EDX analysis.
[h] The relative crystallinity value (%Cryst) calculated by XRD.

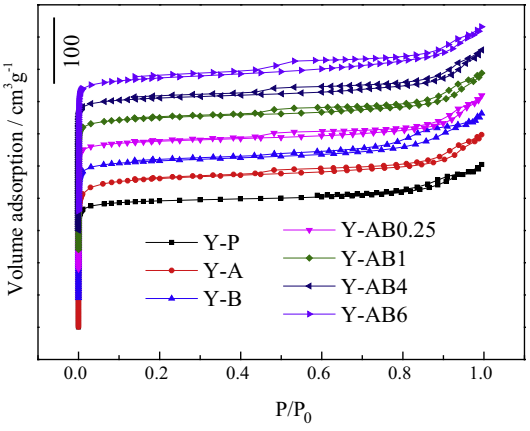

Fig. 3. N_2 sorption isotherms of varied zeolite samples.

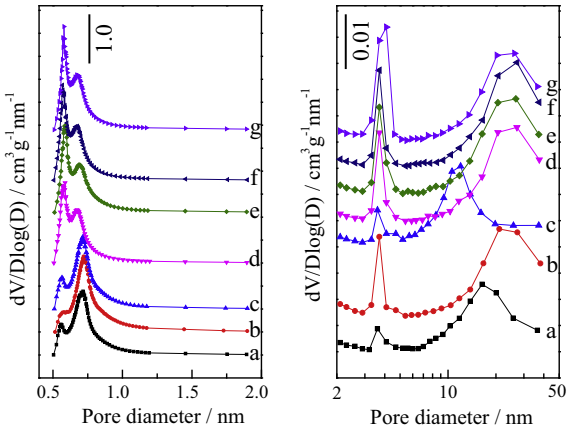

Fig. 4. Pore size distribution of the pristine zeolite (a) Y-P, single acid or base leaching (b) Y-A and (c) Y-B, and hierarchical zeolite (d) Y-AB0.25, (e) Y-AB1, (f) Y-AB4, (g) Y-AB6 (microporous region determined by HK method and mesoporous region determined by BJH method).

enlarges obviously for the single base leaching-treated sample of Y-B. For the Y-AB*x* series samples prepared by the combination of acid leaching and base leaching, their hysteresis loop scopes enlarge gradually with increasing the base leaching time from 0.25 to 6 h, suggesting the pore sizes enlarge gradually by increasing the base leaching time.

The pore size distribution of the Y-P, Y-A, Y-B and hierarchical zeolite Y-AB*x* are displayed in Fig. 4. The pristine zeolite Y has a bimodal pore distribution around 0.56 and 0.71 nm in microporous region. For the sample of Y-A prepared by single acid leaching, the peak intensity of its micropore at 0.56 nm is lower than that of Y-P, while the intensity of the peak at 0.71 nm enhances significantly. For the single base leaching treated sample, the obtained Y-B shows slight increase both at 0.56 nm and 0.71 nm in comparison with the Y-P. By using the combination method that consists of the precedent acid leaching and the followed base leaching on the Y-P, the Y-AB*x* zeolite samples were prepared. These samples also exhibit a bimodal pore distribution, but the larger micropore at 0.71 nm shifts negatively to smaller pore size of 0.69 nm. Different from Y-P or Y-B, the peak intensity of 0.56 nm pore becomes larger than that of 0.69 nm pore. The pore distribution of different samples in mesoporous region is also given in Fig. 4. According to the analysis results, two pore sizes in mesoporous region are found in all of the samples. For the pristine Y-P zeolite, two types of mesopores appear at 3.6 nm and 16.4 nm respectively. After single acid leaching, the Y-A sample shows higher intensity at the peak of 3.6 nm and larger pores around 25 nm compared with Y-P. However, the Y-B sample after single base leaching exhibits different pores at 3.6 nm and 12.0 nm, and the last pores are slightly smaller than the counterpart pores of Y-P. For hierarchical zeolite Y-AB*x* ($x = 0.25$, 1, 4 or 6), all of peaks both on size and intensity enlarge clearly compared with that of Y-P sample. The intensity of the peaks increases linearly with increasing the base leaching time. These results suggest that the hierarchical mesopores on zeolite Y can be generated effectively by using the combination of the acid leaching combined with base leaching. Moreover, changing base leaching time is an effective way to control the micro- and mesopores properties of zeolite, forming hierarchical zeolite structure.

The BET surface area, pore volume, Si/Al ratio and relative crystallinity of the pristine zeolite Y-P, Y-A, Y-B and hierarchical zeolite Y-AB*x* ($x = 0.25$, 1, 4 or 6) are listed in Table 1. The mesopore surface area and mesopore volume of the Y-P catalyst are 61 m^2/g and 0.10 m^3/g respectively, indicating the existence of few mesopores possibly derived from the intergranular holes of zeolite. In comparison with pristine Y-P, the BET surface area and total pore volume of Y-A (acid leaching) and Y-B (base leaching) increase obviously. By employing base leaching on the Y-A sample for certain time (0.25, 1, 4 or 6 h), the mesopore surface area and mesopore volume of the obtained Y-AB*x* samples also increase, suggesting more mesopores were created within the Y-P zeolite by the sequential acid and base leaching process. Acid leaching

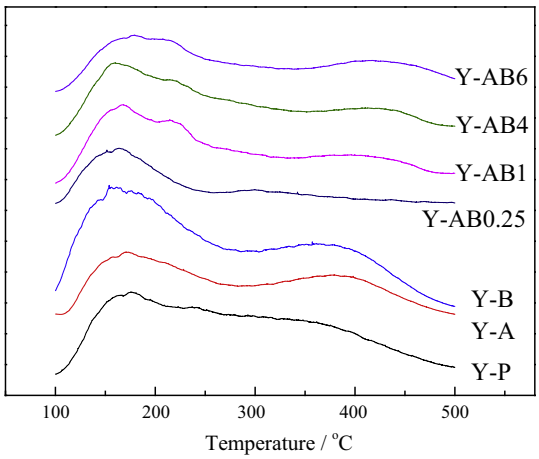

Fig. 5. NH_3-TPD curves of the prepared samples.

for preparing Y-A leads to the selective dealumination of zeolite. Therefore the Si/Al ratio of Y-A increased to 4.92, which is higher than the Si/Al ratio of 3.04 of the Y-P zeolite as indicated in Table 1. Reversely, after the base leaching that can result in the selective desilication of zeolite, the Si/Al ratio of Y-AB*x* series samples decreases gradually along with increasing the base leaching time.

The acidic properties of the prepared samples are measured by NH_3-TPD. The NH_3-TPD profiles of the Y-P, Y-A, Y-B and Y-AB*x* are compared in Fig. 5. The pristine zeolite Y-P exhibits a broad NH_3 desorption peak. The peak starts at a lower temperature about 180 °C, which is associated with the weak acid sites and terminal silanol groups [44]. The higher temperature peak around 420 °C is attributed to some strong Brønsted and Lewis acid sites. After single acid or base leaching on Y-P, the middle acid sites on both of the prepared Y-A and Y-B zeolite decrease obviously as compared with that of Y-P, but the higher acid sites at 420 °C still exist without obvious change. For Y-AB*x* series catalysts, increasing the base leaching time can clearly decrease the amount of acid sites including the middle acid sites and strong acid sites above 250 °C. With these Y-AB*x* zeolite as cobalt supports for FTS reaction, their unique acidic properties together with hierarchical structure should exert considerable effects on the catalytic activity and products distribution [45].

The type and concentration of Brønsted acid sites and Lewis acid sites in the catalyst were determined by Py-IR and illustrated in Fig. 6. The absorption peaks at about 1540 and 1450 cm^{-1} correspond to the Brønsted acid sites and Lewis acid sites, respectively, indicating the coexistence of Brønsted and Lewis acid sites on all the catalysts [46]. And the bands at 1490 cm^{-1} are assigned to pyridine adsorption on both Lewis and Brønsted acid sites [47]. According to the bands assignments, both Brønsted and Lewis acid sites decrease obviously after leaching. It is worth noting that strong Brønsted acid sites to Lewis acid sites (B/L = 8.96, see Table 2) of base leaching zeolite Y (Y-B) are stronger than that of other samples, indicating Brønsted acid sites on Y-B are present predominantly on the zeolite. In addition, the bands of AB*x* samples appear at 1440 cm^{-1}, while the Lewis acid sites shift to 1450 cm^{-1} with the increase of desorption temperature. The result indicates that the total lewis acid sites increases after the combination of acid and base leaching [48].

The acid strength distributions of the Y-P and treated zeolite Y with the pyridine adsorbed IR spectra at 150 and 350 °C are listed

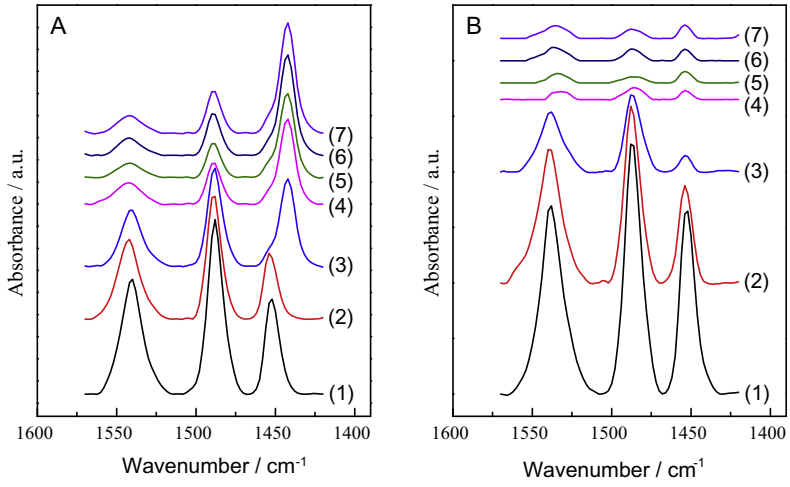

Fig. 6. Py-IR absorbance profiles for the different samples (A) 150 °C and (B) 350 °C: (1) Y-P, (2) Y-A, (3) Y-B, (4) Y-AB0.25, (5) Y-AB1, (6) Y-AB4, (7) Y-AB6.

Table 2
Brønsted acid sites and Lewis acid sites of samples by IR spectra of absorbed pyridine.

Sample	Brønsted acid sites/(μ mol/g)		Lewis acid sites/(μ mol/g)		B/L[a]	
	150	350	150	350	Strong	Total
Y-P	389.4	276.3	161.7	132.4	2.09	2.41
Y-A	282.3	205.0	107.8	61.6	3.33	2.62
Y-B	189.3	86.3	176.3	9.6	8.96	1.07
Y-AB0.25	89.0	8.5	166.4	4.8	1.77	0.53
Y-AB1	55.9	9.6	168.1	6.6	1.46	0.33
Y-AB4	62.2	18.2	195.9	5.8	3.14	0.32
Y-AB6	68.8	20.3	221.0	7.3	2.78	0.31

[a] The number of acid sites is a relative value of Brønsted acid sites to Lewis acid sites, estimated by the corresponding calibrated peak area.

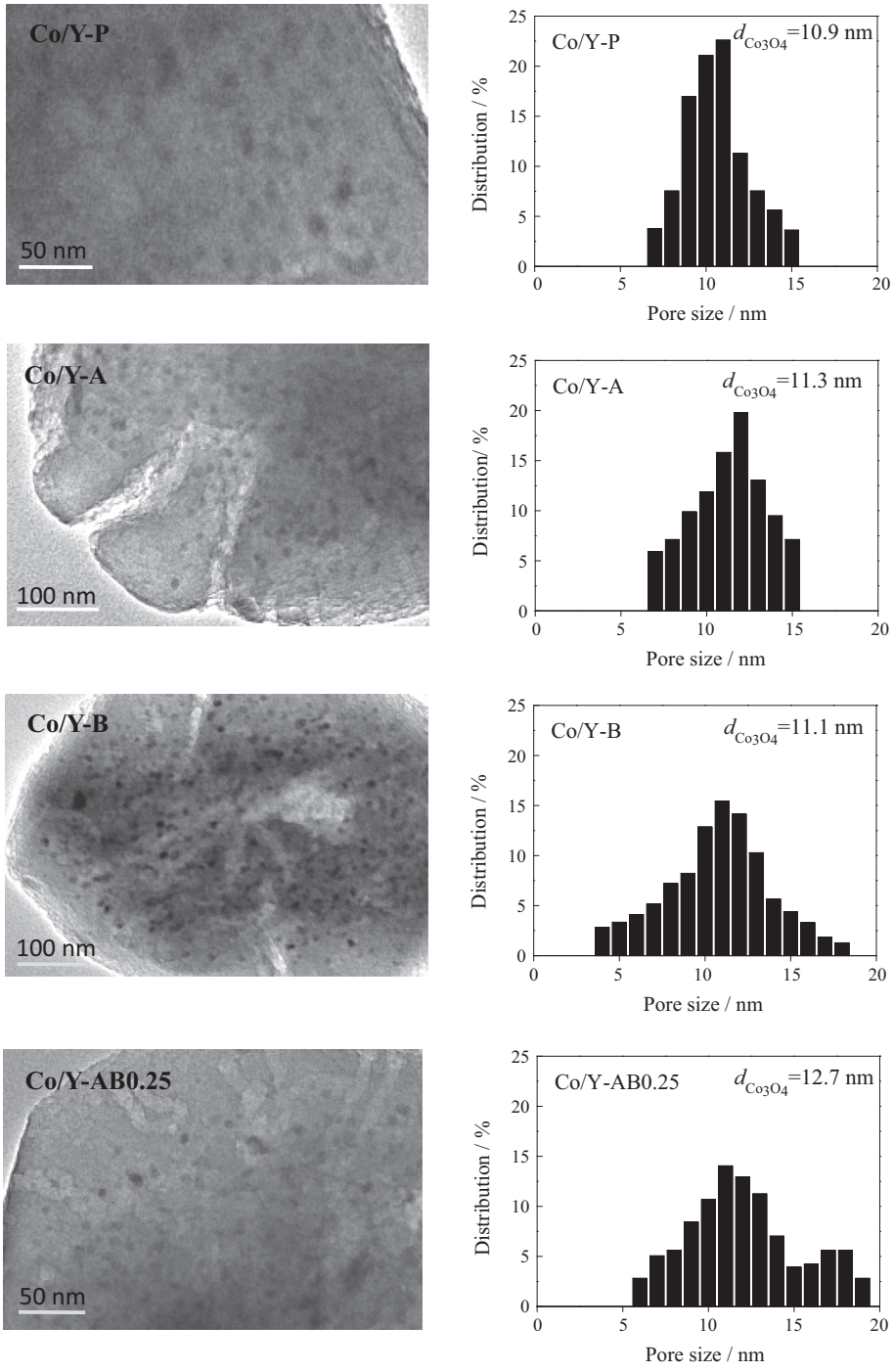

Fig. 7. TEM images and particle size distribution of the different catalysts.

in Table 2. The Y-P sample exhibits the strong strength of Brønsted acid sites and Lewis acid sites. For the base leaching, especially the combination of acid and base leaching, the ratio of total B/L decreases significantly. But the strong B/L obtained from Py-IR at 350 °C enhances obviously for Y-A, Y-B and Y-AB4 samples. It is well known that zeolite Y as an efficient cracking catalyst is applied widely in the conversion of crude oil to transportation fuels because of its strong Brønsted acid sites [49]. The enhanced strong Brønsted acid sites can make effects on catalytic performance and products distribution.

The above zeolite samples are used as supports to prepare cobalt loaded catalysts. The TEM images and particle size distribution of the Co loaded Y-P and hierarchical zeolite are shown in Fig. 7. A small number of mesopores are introduced into the pristine zeolite by acid leaching (Y-A) or base leaching (Y-B). The average diameter of Co_3O_4 on the Co/Y-P, Co/Y-A, Co/Y-B and Co/Y-AB*x* catalysts is measured by TEM observation. The size of Co_3O_4 particles is distributed in the range of 4–19 nm. In addition, a broad particle size distribution is observed with Co/Y-B catalyst. With increasing the NaOH leaching time from 0.25 to 6 h on Y-A for the preparation of hierarchical zeolite Y samples (Y-AB*x*), the mesoporous channels increase significantly, which is an important effect on the promoting diffusion behavior of reactants and products in catalytic process. By sequential dealumination by citric acid and desilication

by NaOH solution for 4 h on Y-P, mesoporous zeolite supported Co catalyst (Co/Y-AB4), shows a smallest Co_3O_4 average particle size with 10.7 nm, smaller than that of other catalysts. However, when the NaOH leaching time is increased to 6 h, the zeolite grains collapse slightly, which is in good agreement with the previous report [50].

The reduction behaviors of the calcined Co/Y-P, Co/Y-A, Co/Y-B and hierarchical zeolite Y supported Co catalysts (Co/Y-AB*x*) are studied using H_2-TPR, as shown in Fig. 8. The H_2-TPR profiles for all catalysts exhibit two major reduction peaks with the temperature in 250–310 °C and 310–500 °C, respectively. The first reduction peak is ascribed to the reduction of Co_3O_4 to CoO. The second reduction peak belongs to the reduction of CoO to Co^0 [51,52]. It can be found that the reduction step from Co_3O_4 to CoO happens quickly, giving a sharp low-temperature peak, while the reduction step from CoO to Co^0 proceeds slowly to form a broad profile [53]. Moreover, different from other samples, the Co/Y-B catalyst exhibits a considerably broad reduction peak above 310 °C, possibly due to its wide Co particle size distribution ranging from 4 to 18 nm (see Fig. 7).

In FTS reaction on these zeolite supported cobalt catalysts, the syngas diffuses in catalysts and reacts initially on the cobalt active sites to form primary FTS products. The formed heavy hydrocarbons escape from catalyst slowly and have more chance to contact the acid sites of zeolite supports, whereby to be converted into light isoparaffin through hydrocracking and isomerization reactions. As well known, the hierarchical structure of the catalyst has important effect on the diffusion behaviors of the reactants and products in catalytic process, which certainly affects the FTS catalysts activity and products selectivity [54]. The FTS reaction performed on the cobalt loaded Y-P, Y-A, Y-B and the hierarchical Y-AB*x* zeolite catalysts are presented in Table 3. The hierarchical structure of zeolite Y with different acid type, strength and amount, and their supported Co catalysts have important effect on the diffusion behaviors of the reactants and products in catalytic process, which certainly affect the FTS activity and products selectivity. On zeolite loaded cobalt catalyst, as bifunctional catalyst system, the primary linear hydrocarbons formed on the FT active metal may undergo several secondary reactions (e.g., the isomerization of the linear hydrocarbons, the hydrocracking of heavier hydrocarbons, and the oligomerizations of the light olefin) on the acid sites. CO conversion obtained on the Co/Y-P catalyst is 50.2%, being accompanied by the formation of some middle isoparaffin. The Co/Y-A and Co/Y-B catalysts treated either acid leaching or base leaching zeolite as supports give CO conversion of 66.2% (Co/Y-A) and 69.7% (Co/Y-B), respectively, higher than that of Co/Y-P catalyst. Meanwhile, the isoparaffin selectivity on

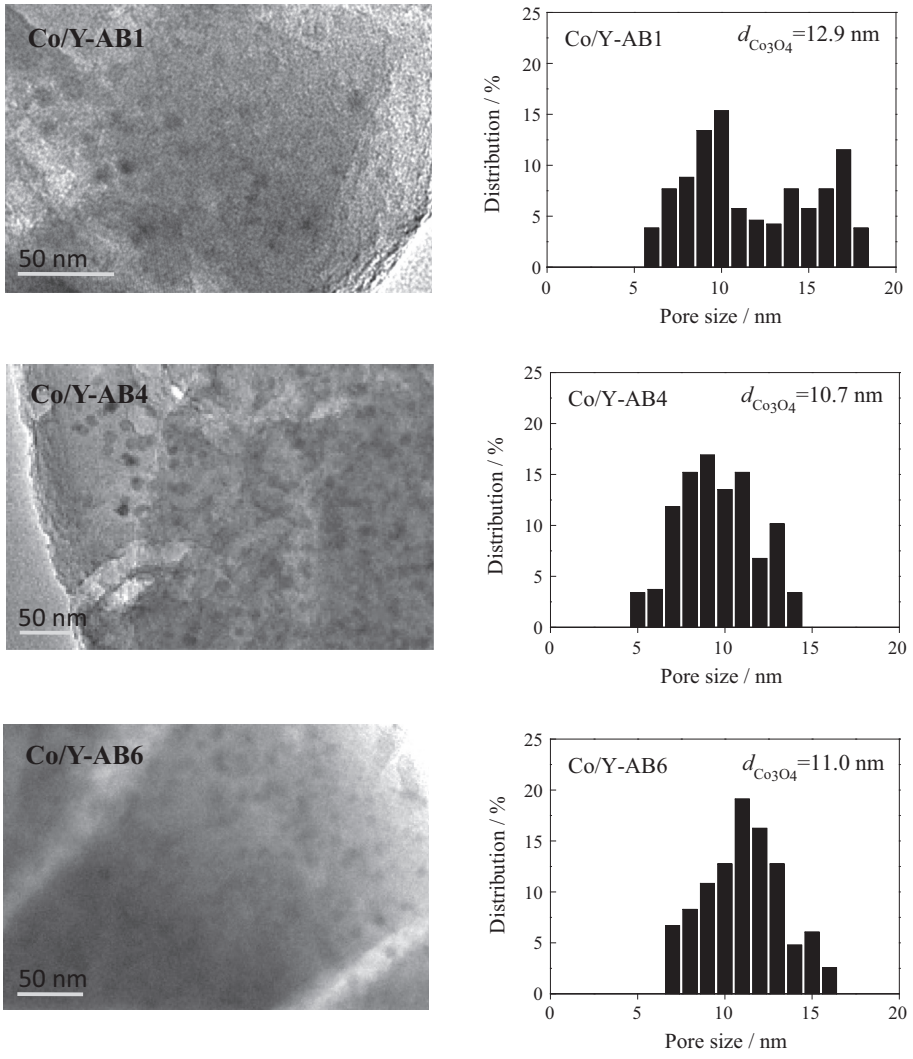

Fig. 7 (*continued*)

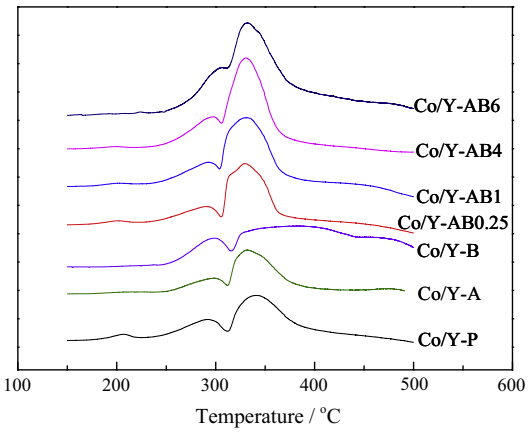

Fig. 8. H_2-TPR curves of the prepared catalysts.

these two catalysts also enhance clearly in comparison with that of Co/Y-P. The improved catalyst activity together with isoparaffin selectivity, here, can be attributed to the well-performed secondary reactions, including hydrocracking and isomerization of the primary FTS products, over mesoporous zeolite supports [55]. The FTS reaction first happens on the Co particles on zeolite supports. And then the formed heavy hydrocarbons diffuse to the acid sites of zeolite supports where they are hydrocracked and isomerized to form light middle isoparaffin. Moreover, the selectivity of unwanted CH_4 on Co/Y-A and Co/Y-B catalyst is only 10.8% and 11.9%, respectively, which is considerably lower than of Co/Y-P with 21.9%. This result can be explained by the known relationship between FTS and catalyst support. The Co/Y-P with more microporous cavities, favors the formation of CH_4 in FTS reaction. And reversely, the mesoporous pores of Y-A and Y-B can depress CH_4 selectivity [56]. Wang et al. concluded that the weaker Lewis acid sites of HZSM-5 were beneficial to the selective production of C_{5-11} hydrocarbons during the hydrocracking of primary FTS products [26]. However, different from reported HZSM-5, zeolite Y as an efficient hydrocracking and isomerization catalyst is attributed to the presence of strong Brønsted acid sites in the zeolite [57]. According to Table 2, the strong B/L ratio of Y-A is 3.33. It supported Co catalyst (Co/Y-A) exhibits a higher isoparaffin selectivity of 50.9% higher than that of Y-P. The Y-B gives the highest strong B/L ratio, but it shows a lower isoparaffin selectivity than Y-A. The result is possibly due to occur the overcracking of primary FTS hydrocarbons on the surface of Y-B with strong Brønsted acid sites.

The CO conversion and hydrocarbons selectivity of FTS reaction performed on the cobalt loaded hierarchical zeolite Y-AB*x* catalysts are also compared in Table 3. The CO conversion on the Co/Y-AB*x* catalysts increases gradually with the increase of base leaching time from 0.25 to 4 h, but the methane selectivity decreases slightly, indicating that more mesopores of zeolite supports facilitate the diffusion of syngas and products, simultaneously suppressing the formation of methane. The CO_2 selectivity obtained by these Co/Y-AB*x* series catalysts is stable, indicating a very low water–gas shift reaction activity under the reaction conditions. However, for Co/Y-AB6 catalyst prepared by longer base leaching time of 6 h, CO conversion decreases suddenly, which is attributed to the partial collapse of zeolite structure during excessive base leaching time, leading lower crystallinity (48.3%). The results indicate that a volcano-like trend of CO conversion and product distribution is obtained for the hierarchical zeolite supported Co catalysts system.

Hierarchical zeolite Y with different pore structure, as catalyst supports, can lead to the varied Co-based FTS catalyst, ultimately tuning the FTS products distribution as we desire. To our studied samples as given in Table 3, it is clear that the light hydrocarbons of C_{2-4} on the Co/Y-AB*x* series catalysts are lower than those of Co/Y-P, Co/Y-A and Co/Y-B catalysts. Strengthening the hierarchical structure of the zeolite with the combined acid and based leaching method (see Fig. 4) possibly weakens the effect of the zeolite Y micropores, finally suppressing the formation of light hydrocarbons in FTS reaction. On the other hand, due to the increase of mesopores on the zeolite supports, the selectivity of C_{5-11} and C_{12+} obtained on Co/Y-AB*x* catalysts increases clearly compared with that of Co/Y-P. These results suggest that the increased pore size of mesoporous zeolite Y support leads to the formation of hydrocarbons toward those with higher carbon number, being in agreement with Khodakov's report [58].

In FTS reaction, zeolite Y acts not only as a support but also an excellent hydrocracking and isomerization catalyst owing to its acid sites, special pores, cavities and regular channels. Reaction results in Table 3 show that isoparaffin can be directly synthesized via FTS reaction using the Co/Y-A, Co/Y-B and Co/Y-AB*x* catalysts. The isoparaffin selectivity enhances obviously with increasing the base leaching time on acid treated zeolite support (Y-AB*x*). The Co/Y-AB4 exhibits the highest isoparaffin selectivity of 52.3% among the tested catalysts because of high strong B/L ratio (3.14) and hierarchical structure as well. As compared with Y-AB4, both Y-A and Y-B have a higher strong B/L ratio, but the surface and volume of mesopores are lower than that of Y-AB4. The results indicate that the strong B/L ratio and textural property are effective for improved FTS activity and isoparaffin selectivity. The product distribution of FTS reaction over Co/Y-P, Co/Y-A, Co/Y-B and Co/Y-AB*x* series catalysts is presented in Fig. 9. Generally, FTS products are normal aliphatic hydrocarbons with few olefin and isoparaffin. However, using the Co/Y-ABx catalysts with varied hierarchical zeolite Y as the supports,

Table 3
Catalytic performance of the pristine and hierarchical zeolite Y supported cobalt catalysts.[a]

Catalyst	Conv./%	Sel./%								
	CO	CO_2	CH_4	C_{2-4}	C_{5-11}	C_{12+}	C_n	$C_=$	C_{iso}	C_{iso}/C_n[b]
Co/Y-P	50.2	1.1	21.9	13.6	59.2	5.3	51.7	18.6	29.8	1.40
Co/Y-A	66.2	1.5	10.8	13.9	69.4	3.4	41.9	7.3	50.9	1.97
Co/Y-B	69.7	2.9	11.9	13.6	65.2	9.3	46.4	10.1	43.5	1.47
Co/Y-AB0.25	66.3	1.9	14.7	10.7	67.6	7.0	46.0	18.1	35.9	1.46
Co/Y-AB1	75.7	3.5	11.4	10.2	67.0	11.4	39.1	18.2	42.6	1.89
Co/Y-AB4	75.9	1.8	8.4	7.7	71.8	12.1	29.5	18.3	52.3	3.06
Co/Y-AB6	66.5	2.0	14.5	12.8	65.0	7.7	46.2	13.9	39.9	1.58

[a] Reaction conditions: catalyst 0.5 g; temperature 260 °C; pressure 1.0 MPa; H_2/CO_2; $W_{Catalyst}/F_{Syngas}$ 10 g h/mol.
[b] C_{iso}/C_n is the ratio of isoparaffin to paraffin of C_{4+}.

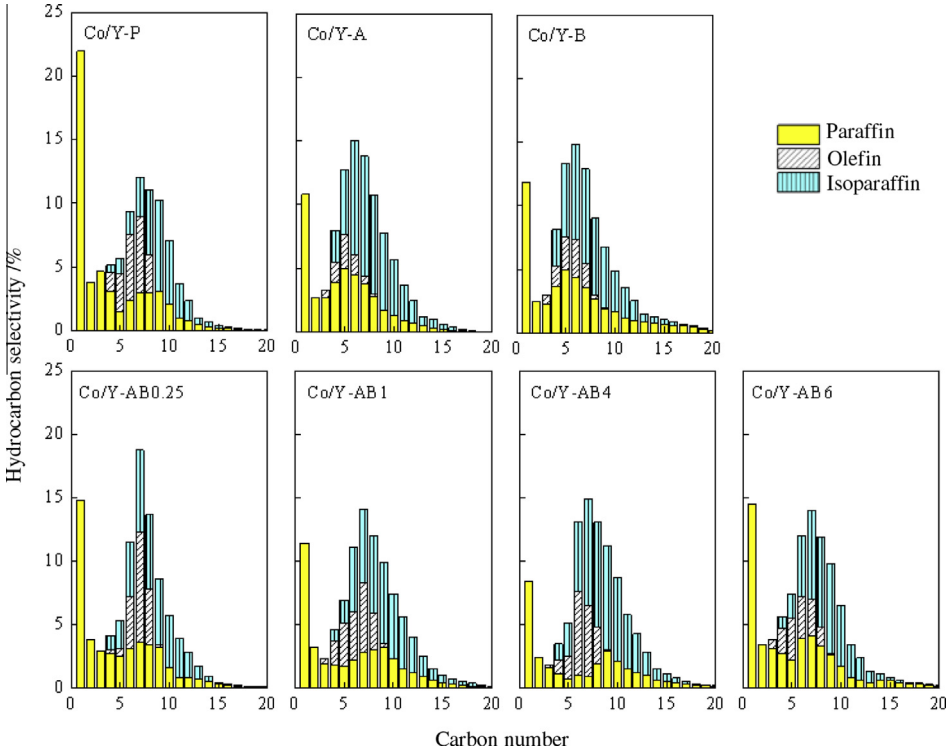

Fig. 9. Product distribution of FTS reaction performance on the Co/Y-P, Co/Y-A, Co/Y-B and Co/Y-AB*x* catalysts.

the product selectivity, especially isoparaffin selectivity, can be facilely tuned with the restrained formation of light hydrocarbons of C_{1-4} simultaneously.

4. Conclusions

Hierarchical zeolite Y with intra-crystalline mesopores was obtained facilely by a sequential acid and base leaching method. By increasing the base leaching time from 0.25 to 6 h on the acid-leached Y-A zeolite, the obtained Y-AB*x* (x = 0.25, 1, 4 and 6) samples exhibited high mesopore surface area and volume as compared with the pristine zeolite Y. With the obtained hierarchical zeolite Y as supports, we prepared a series of cobalt loaded catalysts for FTS reaction to investigate the effect of supports hierarchical structure on tuning FTS products distribution. The CO conversion and C_{5+} selectivity of the hierarchical zeolite Y supported Co catalysts were much higher than that of untreated zeolite support cobalt catalyst (Co/Y-P). Especially on Co/Y-AB4 catalyst, due to the optimized hydrocracking and isomerization function afforded by the hierarchical zeolite structure and high B/L ratio, isoparaffin with the highest selectivity of 52.3% became the main FTS products instead of the general FTS products of normal paraffin. Facilely tuning the FTS product distribution, especially the content of isoparaffin, could be realized using the hierarchical zeolite Y supported cobalt as catalysts. The presented hierarchical zeolite Y preparation method and its application for tuning the FTS product distribution reported here will further inspire the development of zeolite-based catalyst for FTS reaction to synthesize directly the desired hydrocarbons more efficiently.

Acknowledgements

The authors acknowledge the financial support from Zhejiang Province Natural Science Foundation (LY14B030004). And we also thank the Japan–China joint research fund on coal utilization from JST-MOST.

References

[1] van Donk S, Janssen AH, Bitter JH, de Jong KP. Generation, characterization, and impact of mesopores in zeolite catalysts. Catal Rev 2003;45:297–319.
[2] Coelho A, Caeiro G, Lemos MANDA, Lemos F, Ribeiro FR. 1-Butene oligomerization over ZSM-5 zeolite: part 1 – effect of reaction conditions. Fuel 2013;111:449–60.
[3] Echeandia S, Pawelec B, Barrio VL, Arias PL, Cambra JF, Loricera CV, et al. Enhancement of phenol hydrodeoxygenation over Pd catalysts supported on mixed HY zeolite and Al_2O_3. An approach to O-removal from bio-oils. Fuel 2014;117:1061–73.
[4] Groen JC, Abello S, Villaescusa LA, Perez-Ramirez J. Mesoporous beta zeolite obtained by desilication. Micropor Mesopor Mater 2008;114:93–102.
[5] Guo YP, Wang HJ, Guo YJ, Guo LH, Chu LF, Guo CX. Fabrication and characterization of hierarchical ZSM-5 zeolites by using organosilanes as additives. Chem Eng J 2011;166:391–400.
[6] Groen JC, Peffer LAA, Moulijn JA, Perez-Ramirez J. Mesoporosity development in ZSM-5 zeolite upon optimized desilication conditions in alkaline medium. Colloid Surf A Physicochem Eng Aspects 2004;241:53–8.
[7] de Jong KP, Zecevic J, Friedrich H, de Jongh PE, Bulut M, van Donk S, et al. Zeolite Y crystals with trimodal porosity as ideal hydrocracking catalysts. Angew Chem Int Ed 2010;49:10074–8.
[8] He T, Wang Y, Miao P, Li J, Wu J, Fang Y. Hydrogenation of naphthalene over noble metal supported on mesoporous zeolite in the absence and presence of sulfur. Fuel 2013;106:365–71.
[9] Abbasov V, Mammadova T, Andrushenko N, Hasankhanova N, Lvov Y, Abdullayev E. Halloysite-Y-zeolite blends as novel mesoporous catalysts for the cracking of waste vegetable oils with vacuum gasoil. Fuel 2014;117:552–5.
[10] Meng X, Nawaz F, Xiao FS. Templating route for synthesizing mesoporous zeolites with improved catalytic properties. Nano Today 2009;4:292–301.
[11] Aguado J, Serrano DP, Escola JM, Briones L. Deactivation and regeneration of a Ni supported hierarchical Beta zeolite catalyst used in the hydroreforming of the oil produced by LDPE thermal cracking. Fuel 2013;109:679–86.
[12] Fathi S, Sohrabi M, Falamaki C. Improvement of HZSM-5 performance by alkaline treatments: comparative catalytic study in the MTG reactions. Fuel 2014;116:529–37.
[13] Sasaki Y, Suzuki T, Takamura Y, Saji A, Saka H. Structure analysis of the mesopore in dealuminated zeolite Y by high resolution TEM observation with slow scan CCD camera. J Catal 1998;178:94–100.
[14] White RJ, Fischer A, Goebel C, Thomas A. A sustainable template for mesoporous zeolite synthesis. J Am Chem Soc 2014;136:2715–8.
[15] Xue C, Zhang F, Wu L, Zhao D. Vapor assisted "in situ" transformation of mesoporous carbon–silica composite for hierarchically porous zeolites. Micropor Mesopor Mater 2012;151:495–500.
[16] Cho HS, Ryoo R. Synthesis of ordered mesoporous MFI zeolite using CMK carbon templates. Micropor Mesopor Mater 2012;151:107–12.

[17] Wang X, Li G, Wang W, Jin C, Chen Y. Synthesis, characterization and catalytic performance of hierarchical TS-1 with carbon template from sucrose carbonization. Micropor Mesopor Mater 2011;142:494–502.
[18] Chen LH, Li XY, Rooke JC, Zhang YH, Yang XY, Tang Y, et al. Hierarchically structured zeolites: synthesis, mass transport properties and applications. J Mater Chem 2012;22:17381–403.
[19] Chal R, Gerardin C, Bulut M, van Donk S. Overview and industrial assessment of synthesis strategies towards zeolites with mesopores. ChemCatChem 2011;3:67–81.
[20] Chu N, Yang J, Li C, Cui J, Zhao Q, Yin X, et al. An unusual hierarchical ZSM-5 microsphere with good catalytic performance in methane dehydroaromatization. Micropor Mesopor Mater 2009;118:169–75.
[21] Su L, Liu L, Zhuang J, Wang H, Li Y, Shen W, et al. Creating mesopores in ZSM-5 zeolite by alkali treatment: a new way to enhance the catalytic performance of methane dehydroaromatization on Mo/HZSM-5 catalysts. Catal Lett 2003;91:155–67.
[22] Li X, Prins R, van Bokhoven JA. Synthesis and characterization of mesoporous mordenite. J Catal 2009;262:257–65.
[23] Sartipi S, van Dijk JE, Gascon J, Kapteijn F. Toward bifunctional catalysts for the direct conversion of syngas to gasoline range hydrocarbons: H-ZSM-5 coated Co versus H-ZSM-5 supported Co. Appl Catal A Gen 2013;456:11–22.
[24] Sartipi S, Parashar K, Valero-Romero MJ, Santos VP, van der Linden B, Makkee M, et al. Hierarchical H-ZSM-5-supported cobalt for the direct synthesis of gasoline-range hydrocarbons from syngas: advantages, limitations, and mechanistic insight. J Catal 2013;305:179–90.
[25] Sartipi S, Parashar K, Makkee M, Gascon J, Kapteijn F. Breaking the Fischer–Tropsch synthesis selectivity: direct conversion of syngas to gasoline over hierarchical Co/H-ZSM-5 catalysts. Catal Sci Technol 2013;3:572–5.
[26] Kang JC, Cheng K, Zhang L, Zhang QH, Ding JS, Hua WQ, et al. Mesoporous zeolite-supported ruthenium nanoparticles as highly selective Fischer–Tropsch catalysts for the production of C5–C11 isoparaffins. Angew Chem Int Ed 2011;50:5200–3.
[27] Yang G, He J, Zhang Y, Yoneyama Y, Tan Y, Han Y, et al. Design and modification of zeolite capsule catalyst, a confined reaction field, and its application in one-step isoparaffin synthesis from syngas. Energy Fuel 2008;22:1463–8.
[28] Bao J, He J, Zhang Y, Yoneyama Y, Tsubaki N. A core/shell catalyst produces a spatially confined effect and shape selectivity in a consecutive reaction. Angew Chem Int Ed 2008;47:353–6.
[29] Xing C, Yang G, Wang D, Zeng C, Jin Y, Yang R, et al. Controllable encapsulation of cobalt clusters inside carbon nanotubes as effective catalysts for Fischer–Tropsch synthesis. Catal Today 2013;215:24–8.
[30] Fu T, Huang C, Lv J, Li Z. Fuel production through Fischer–Tropsch synthesis on carbon nanotubes supported Co catalyst prepared by plasma. Fuel 2014;121:225–31.
[31] Di Fronzo A, Pirola C, Comazzi A, Galli F, Bianchi CL, Di Michele A, et al. Co-based hydrotalcites as new catalysts for the Fischer–Tropsch synthesis process. Fuel 2014;119:62–9.
[32] He J, Xu B, Yoneyama Y, Nishiyama N, Tsubaki N. Designing a new kind of capsule catalyst and its application for direct synthesis of middle isoparaffins from synthesis gas. Chem Lett 2005;34:148–9.
[33] Zhang Q, Kang J, Wang Y. Development of novel catalysts for Fischer–Tropsch synthesis: tuning the product selectivity. ChemCatChem 2010;2:1030–58.
[34] Wang YL, Hou B, Chen JG, Jia LT, Li DB, Sun YH. Ethylenediamine modified Co/SiO_2 sol–gel catalysts for non-ASF FT synthesis of middle distillates. Catal Commun 2009;10:747–52.
[35] Huang X, Hou B, Wang J, Li D, Jia L, Chen J, et al. CoZr/H-ZSM-5 hybrid catalysts for synthesis of gasoline-range isoparaffins from syngas. Appl Catal A Gen 2011;408:38–46.
[36] Ngamcharussrivichai C, Liu X, Li X, Vitidsant T, Fujimoto K. An active and selective production of gasoline-range hydrocarbons over bifunctional Co-based catalysts. Fuel 2007;86:50–9.
[37] Li J, Tan Y, Zhang Q, Han Y. Characterization of an HZSM-5/MnAPO-11 composite and its catalytic properties in the synthesis of high-octane hydrocarbons from syngas. Fuel 2010;89:3510–6.
[38] Corma A. Inorganic solid acids and their use in acid-catalyzed hydrocarbon reactions. Chem Rev 1995;95:559–614.
[39] Mante OD, Agblevor FA, McClung R. A study on catalytic pyrolysis of biomass with Y-zeolite based FCC catalyst using response surface methodology. Fuel 2013;108:451–64.
[40] Mante OD, Agblevor FA, Oyama ST, McClung R. Catalytic pyrolysis with ZSM-5 based additive as co-catalyst to Y-zeolite in two reactor configurations. Fuel 2014;117:649–59.
[41] Emeis C. Determination of integrated molar extinction coefficients for infrared absorption bands of pyridine adsorbed on solid acid catalysts. J Catal 1993;141:347–54.
[42] Tarach K, Góra-Marek K, Tekla J, Brylewska K, Datka J, Mlekodaj K, et al. Catalytic cracking performance of alkaline-treated zeolite Beta in the terms of acid sites properties and their accessibility. J Catal 2014;312:46–57.
[43] Verboekend D, Vile G, Perez-Ramirez J. Mesopore formation in USY and beta zeolites by base leaching: selection criteria and optimization of pore-directing agents. Cryst Growth Des 2012;12:3123–32.
[44] Taufiqurrahmi N, Mohamed AR, Bhatia S. Nanocrystalline zeolite beta and zeolite Y as catalysts in used palm oil cracking for the production of biofuel. J Nanopart Res 2011;13:3177–89.
[45] Tao H, Yang H, Liu X, Ren J, Wang Y, Lu G. Highly stable hierarchical ZSM-5 zeolite with intra- and inter-crystalline porous structures. Chem Eng J 2013;225:686–94.
[46] Tan Q, Bao X, Song T, Fan Y, Shi G, Shen B, et al. Synthesis, characterization, and catalytic properties of hydrothermally stable macro–meso–micro-porous composite materials synthesized via in situ assembly of preformed zeolite Y nanoclusters on kaolin. J Catal 2007;251:69–79.
[47] Zhang Q, Wang TJ, Xu Y, Zhang Q, Ma LL. Production of liquid alkanes by controlling reactivity of sorbitol hydrogenation with a Ni/HZSM-5 catalyst in water. Energy Convers Manage 2014;77:262–8.
[48] Zhu Z, Chen Q, Xie Z, Yang W, Li C. The roles of acidity and structure of zeolite for catalyzing toluene alkylation with methanol to xylene. Micropor Mesopor Mater 2006;88:16–21.
[49] Williams B, Babitz S, Miller J, Snurr R, Kung H. The roles of acid strength and pore diffusion in the enhanced cracking activity of steamed Y zeolites. Appl Catal A Gen 1999;177:161–75.
[50] Ogura M, Shinomiya SY, Tateno J, Nara Y, Nomura M, Kikuchi E, et al. Alkali-treatment technique-new method for modification of structural and acid-catalytic properties of ZSM-5 zeolites. Appl Catal A Gen 2001;219:33–43.
[51] Mu SF, Li DB, Hou B, Jia LH, Chen JG, Sun YH. Influence of ZrO(2) loading on SBA-15-Supported cobalt catalysts for Fischer–Tropsch synthesis. Energy Fuel 2010;24:3715–8.
[52] Sun J, Niu W, Taguchi A, Abe T, Yoneyama Y, Tsubaki N. Combining wet impregnation and dry sputtering to prepare highly-active CoPd/H-ZSM5 ternary catalysts applied for tandem catalytic synthesis of isoparaffins. Catal Sci Technol 2014;4:1260–7.
[53] Xiong H, Zhang Y, Liew K, Li J. Fischer–Tropsch synthesis: the role of pore size for Co/SBA-15 catalysts. J Mol Catal A: Chem 2008;295:68–76.
[54] Zhang X, Tao K, Kubota T, Shimamura T, Kawabata T, Matsuda K, et al. Trimodal pore catalyst preparation method by growth of zeolite inside macroporous matrices of silica. Appl Catal A Gen 2011;405:160–5.
[55] Martinez A, Prieto G. The application of zeolites and periodic mesoporous silicas in the catalytic conversion of synthesis gas. Top Catal 2009;52:75–90.
[56] Sartipi S, Alberts M, Santos VP, Nasalevich M, Gascon J, Kapteijn F. Insights into the catalytic performance of mesoporous H-ZSM-5-supported cobalt in Fischer–Tropsch synthesis. ChemCatChem 2014;6:142–51.
[57] Corma A, Grande M, Gonzalez-Alfaro V, Orchilles A. Cracking activity and hydrothermal stability of MCM-41 and its comparison with amorphous silica-alumina and a USY zeolite. J Catal 1996;159:375–82.
[58] Khodakov AY, Griboval-Constant A, Bechara R, Zholobenko VL. Pore size effects in Fischer Tropsch synthesis over cobalt-supported mesoporous silicas. J Catal 2002;206:230–41.